research articles Journal of proteome research

Systems Metabolic Effects of a *Necator americanus* Infection in Syrian Hamster

Yulan Wang,[†,*] Shu-Hua Xiao,[‡] Jian Xue,[‡] Burton H. Singer,[§] Jürg Utzinger,[#] and Elaine Holmes[||]

State Key Laboratory of Magnetic Resonance and Atomic and Molecular Physics, Wuhan Centre for Magnetic Resonance, Wuhan Institute of Physics and Mathematics, Chinese Academy of Sciences, Wuhan 430071, People's Republic of China, National Institute of Parasitic Diseases, Chinese Center for Disease Control and Prevention, Shanghai 200025, People's Republic of China, Office of Population Research, Princeton University, 245 Wallace Hall, Princeton, New Jersey 08544, Department of Public Health and Epidemiology, Swiss Tropical Institute, P.O. Box, CH-4002 Basel, Switzerland, Department of Biomolecular Medicine, Department of Surgery and Cancer, Faculty of Medicine, Imperial College London, Sir Alexander Fleming Building, South Kensington, London SW7 2AZ, United Kingdom

Received May 4, 2009

Hookworms (*Ancylostoma duodenale* and *Necator americanus*) are blood-feeding intestinal nematodes that infect ~700 million people worldwide. To further our understanding of the systems metabolic response of the mammalian host to hookworm infection, we employed a metabolic profiling strategy involving the combination of ^{1}H NMR spectroscopic analysis of urine and serum and multivariate data analysis techniques to investigate the biochemical consequences of a *N. americanus* infection in the hamster. The infection was characterized by altered energy metabolism, consistent with hookworm-induced anemia. Additionally, disturbance of gut microbiotal activity was associated with a *N. americanus* infection, manifested in the alterations of microbial-mammalian cometabolites, including phenylacetylglycine, *p*-cresol glucuronide, 4-hydroxy-3-methyl-phenylpropionic acid, hippurate, 4-hydroxyphenylactate, and dimethylamine. The correlation between worm burden and metabolite concentrations also reflected a changed energy metabolism and gut microbial state. Furthermore, elevated levels of urinary 2-aminoadipate was a characteristic feature of the infection, which may be associated with the documented neurological consequences of hookworm infection.

Keywords: Hookworm • *Necator americanus* • Hamster • Metabolic Profiling • Microbiota • ^{1}H NMR Spectroscopy • Multivariate Data Analysis

Introduction

Hookworms are small blood-feeding intestinal nematodes. There are two species parasitizing humans, *Ancylostoma duodenale* and *Necator americanus*. Approximately 700 million individuals are infected with hookworms, mainly in the developing world.[1] According to recent estimates, the global burden due to hookworm disease might be as high as 22.1 million disability-adjusted life years.[2] Humans acquire a hookworm infection *via* third stage infective larvae (L_3) penetrating the unbroken skin. The larvae travel to the heart and lung and then move to trachea where they are swallowed. After going through two molts, larvae develop into blood-feeding adult worms, a process which takes 5−9 weeks in humans and ~5 weeks in the laboratory hamster model, whereupon the female worms start to produce eggs that are excreted in the feces. The eggs hatch in moist soil and produce larvae that develop to the L_3 stage after two molts, completing the hookworm life cycle.[3] The main pathology associated with a hookworm infection is anemia and malnutrition, but other known effects include cognitive impairment and growth retardation in children.[1,4−6] In highly endemic areas, the key strategy for the control of hookworm and other common soil-transmitted helminths (i.e., *Ascaris lumbricoides* and *Trichuris trichiura*) relies on large-scale administration of anthelmintic drugs, using mainly albendazole and mebendazole.[7,8] For nearly a century, this deworming strategy has, unfortunately, rarely been accompanied by adequate prevention programs.[9]

Considerable efforts have been made to develop a vaccine against hookworm, and thus far, more than 20 proteins have been explored as potential vaccine antigen targets.[3,10] However, there is still a long way to go before an effective hookworm vaccine might eventually become available. Fundamental research aimed at elucidating the pathogenesis of hookworm infection and interactions between host and parasite may

* Correspondence should be addressed to: Yulan Wang, State Key Laboratory of Magnetic Resonance and Atomic and Molecular Physics, Wuhan Centre for Magnetic Resonance, Wuhan Institute of Physics and Mathematics, Chinese Academy of Sciences, Wuhan 430071, People's Republic of China. Tel, +86 27 8719-7143; fax, +44 27 8719-9291; e-mail, yulan.wang@wipm.ac.cn.
† Wuhan Centre for Magnetic Resonance.
‡ National Institute of Parasitic Diseases.
§ Princeton University.
# Swiss Tropical Institute.
|| Imperial College London.

10.1021/pr900711j CCC: $40.75
Published on Web 10/08/2009

provide valuable information for novel vaccine and drug candidates. Metabolic profiling pursues a systems biology approach and can deepen our understanding of metabolic responses of an organism to stimuli, such as disease, physiological changes, and genetic modification.[11] Typically, metabolic profiling combines high-resolution NMR spectroscopy or mass spectrometry (MS) with chemometric data analysis techniques to generate comprehensive biochemical profiles of the biofluids or tissues of an organism. It is a robust and reproducible method for investigating physiological or pathological perturbations in biological systems, and has been successfully applied to the elucidation of metabolic interactions between host and parasites. The first such application was the characterization of the metabolic fingerprint of a trematode infection (*Schistosoma mansoni*) in the mouse. Stimulated glycolysis, perturbation of tricarboxylic acid cycle intermediates, disturbed amino acid metabolism, and variation in the composition or activities of gut microbiota were prominent changes due to a *S. mansoni* infection.[12] Subsequent applications pertained to a related trematode (*Schistosoma japonicum*) in the hamster,[13] another trematode (*Echinostoma caproni*) in the mouse,[14,15] a nematode (*Trichinella spiralis*) in the mouse,[16] and two protozoa (*Trypanosoma brucei brucei*[17] and *Plasmodium berghei*[18]) in mice.

In the present study, we extended our metabolic profiling strategy to the most significant nematode parasitizing humans (i.e., hookworm) and employed a hamster model.[19] Our aim was to determine the systems metabolic response of the hamster to this nematode with a view to identifying potential metabolic biomarkers that might be harnessed for discovery and development of new diagnostics, drug, and vaccine candidates.

Methods

Hamster Infection and Sample Collection. The study was performed at the National Institute of Parasitic Diseases (IPD), Chinese Center for Disease Control and Prevention (Shanghai, China) according to the guidelines of the Chinese Academy of Science (Shanghai, China; permission no. SCXK(Hu) 2003−0003). A total of 20 male Syrian SLAC hamsters were purchased from Shanghai Animal Centre, Chinese Academy of Science. The hamsters were kept in 4 groups of 5 animals per cage at the animal husbandry of IPD at an ambient temperature of 24−26 °C. All animals had free access to water and standard rodent diet. After 1 week of acclimatization, 10 hamsters were infected subcutaneously with 250 *N. americanus* L_3. The remaining 10 hamsters were kept as uninfected controls.

Urine samples were collected in the morning starting at 08:30 h by placing the hamsters in individual metabolic cages. As soon as 0.5 mL of urine was obtained, the sample was transferred into a freezer and stored at −40 °C. If less than 0.5 mL of urine was produced within 2 h, 2 mL of tap water was orally administered to hamsters once every 30 min for up to 3 times until a sufficiently large amount of urine was obtained. Urine collections were performed at 5 time points, that is, 1 day before infection, and on days 1, 7, 21, and 35 postinfection.

Thirty-five days after infection, hamsters were killed by cervical dislocation without prior anesthesia to avoid potential interference of the anesthesia with the analytical data. Approximately 1 mL of blood was collected into Eppendorf tubes and centrifuged at 5000 *g* for 10 min. Serum was transferred into 1.5 mL Eppendorf tubes, transferred in a freezer and kept at −40 °C.

Hamsters were dissected and adult *N. americanus* worms were collected as follows. In a first step, the intestine and colon were opened and the entire content immersed in a Petri dish filled with saline (0.9%). Worms were removed and counted. Subsequently, worms were systematically searched in the lumen and the intestinal mucosa, removed and counted.

Urine and serum samples were stored in a freezer at −40 °C at the National Institute of Parasitic Diseases, transferred on dry ice to Imperial College London, where they were kept in a freezer at −40 °C pending ^{1}H NMR spectroscopic analyses. The total storage time before NMR experiments were performed was 7 months.

Sample Preparation and ^{1}H NMR Measurement. Urine samples were prepared by adding 0.4 mL aliquot of hamster urine to 0.2 mL of 0.2 M (pH 7.4) phosphate buffer, containing 10% D_2O and 0.05% sodium 3-(trimethylsilyl) propionate-2,2,3,3-d_4 (TSP). Serum samples were prepared by adding 0.2 mL of serum to 0.4 mL of a saline solution containing 10% D_2O and 0.9% NaCl. Samples were centrifuged at 5000 *g* for 5 min and 0.5 mL of the supernatant was pipetted into a 5 mm outer diameter NMR tube. The D_2O served as a field frequency lock.

All NMR spectra were acquired at 300 K on a Bruker DRX 600 MHz NMR spectrometer (Bruker Analytische Messtechnik GmbH; Rheinstetten, Germany) operating at 600.13 MHz, with a triple resonance inverse detection probe and XwinNMR version 3.5 (Bruker Analytische Messtechnik GmbH; Rheinstetten, Germany). A standard one-dimensional (1D) pulse sequence was used for acquiring urine spectra. The water signal was suppressed by a weak irradiation of the water peak during a recycle delay (RD) of 2 s, and mixing time (t_m) of 150 ms. t_1 was set to 3 μs. A total of 64 transients with 32k data points were collected for each spectrum with a spectral width of 20 ppm.

^{1}H NMR spectra of serum samples were recorded with Carr−Purcell−Meibom−Gill (CPMG) spin−echo pulse sequence [RD-90°-(τ-180°-τ)$_n$-ACQ].[20] This pulse sequence enables the suppression of signals from macromolecules and other molecules with constrained molecular motions. A total spin−spin relaxation delay ($2n\tau$) of 160 ms was used for all samples and irradiation of the water signal was applied during the relaxation delay. A total of 128 scans with 32 k data points were accumulated for each serum spectrum. A 90° pulse length was adjusted to ∼10 μs.

To aid metabolite identification, solid phase extraction chromatography was performed for selected samples. Briefly, a C-18 SPE column (Isolute, IST International Sorbent Technology, U.K.) was prewashed with 100% methanol and conditioned with 2% methanol solution before 1 mL of urine sample was loaded onto the column. The urine sample was then eluted with 2%, 5%, 10%, 20%, 30%, 50%, and 100% methanol solution. The methanol was evaporated from the collected fractions followed by freeze-drying. Two-dimensional (2D) NMR was then performed on these samples, including correlation spectroscopy (COSY)[21] and total correlation spectroscopy (TOCSY)[22] using standard acquisition parameters.

NMR Spectral Data Processing and Analysis. All free induction decays (FIDs) were multiplied by an exponential function equivalent to a line broadening of 0.3 Hz prior to Fourier transformation. The spectra were manually phased and baseline-corrected using Topspin (Bruker Analytische Messtechnik GmbH; Rheinstetten, Germany). Spectra obtained from urine were referenced using TSP peak at δ 0.00, whereas those of serum were referenced using the anomeric proton of the

α-glucose resonance at δ 5.223. The spectra over the chemical shift range δ 0.5−8.5 and δ 0.3−8.0 for urine and serum spectra respectively were digitized with an in-house developed MATLAB script. To avoid the effects of imperfect water suppression, the chemical shift ranges δ 4.22−6.15 and δ 4.37−5.15 were removed from urine and serum spectra, respectively. The spectra were then normalized to the total sum of the remaining spectral data prior to data analysis.

Principal component analysis (PCA)[23,24] and orthogonal-projection to latent structure-discriminant analysis (O-PLS-DA) were employed in the analysis of the spectral data.[25] PCA is an unsupervised method and facilitates the visualization of intrinsic similarities and differences between objects (i.e., biofluid samples) within the data set. On the other hand, O-PLS-DA,[25] which is an extension of the partial least-squares regression method[26] featuring an integrated orthogonal signal correction filter, is a supervised method. It uses information relating to the class of objects to maximize the separation between 2 or more classes and to identify the features that systematically differ between those classes.[24] PCA was performed using the SIMCA-P+11 software package (Umetrics; Umeå, Sweden) and O-PLS-DA modeling was carried out on the mean centered data scaled to unit variance prior to analysis using MATLAB version 7.0 with scripts developed at Imperial College London. For visualization purposes, the O-PLS coefficients indicating those variables contributing to the discrimination in the model were back-transformed, as described elsewhere.[27]

The validation of models was conducted using 7-fold cross-validation and permutation testing. A 7-fold cross-validation method was performed *via* iterative construction of models by repeatedly leaving out one-seventh of the samples, and predicting them back into the model.[27] The permutation test was conducted by constructing 20 000 models using randomized classification for the samples and Q^2 values generated from these random models were compared to the Q^2 of real model.[28] Since the classification was randomized, there is a chance that the dummy classification is the same as the actual classification, in which case Q^2 obtained from the permutation test should be equal to the real Q^2 obtained from the model. Hence, only if the maximum value from the permutation test (Q^2_{max}) is smaller than, or equal to, the Q^2 of real model, the model is regarded as a predictive model.

Resonance assignments were aided by the literature,[29] confirmed by 2D COSY and TOCSY ^{1}H NMR spectra and solid phase extraction. Additionally, a statistical total correlation spectroscopy (STOCSY)[30] method was applied as an aid for assigning metabolites. STOCSY takes advantage of linear covariation between different NMR signal intensities derived from the same molecule from samples containing different concentrations of the molecule, providing that NMR spectra were acquired under identical conditions.

Results

Worm Burden. On average, 39 adult *N. americanus* worms were recovered per hamster 35 days postinfection (standard deviation (SD), 14 worms; range, 20−62 worms). The mean numbers of male and female worms were similar (females = 19; males = 20).

^{1}H NMR Spectra of Hamster Urine and Serum. Representative ^{1}H NMR spectra of urine and serum samples obtained from *N. americanus*-infected hamsters, together with spectra derived from uninfected control hamster, are shown in Figures 1 and 2, respectively. The endogenous metabolites detected in the urine spectra consisted of a number of amino acids, such as alanine and taurine, and a range of short chain fatty acids (SCFAs) and amine containing compounds, including butyrate, 2-ketoisocaproate, D-3-hydroxybutyrate, lactate, acetate, succinate, citrate, formate, dimethylamine (DMA), trimethylamine (TMA), dimethylglycine (DMG), and trimethylamine-*N*-oxide (TMAO). Additionally, creatine, creatinine, carnitine, acetylcarnitine and a range of aromatic compounds such as 4-hydroxyphenylacetate, phenylacetylglycine (PAG), hippurate, *p*-cresol-glucuronide, and 4-hydroxy-3-methylphenylpropionic acid were found in urine spectra of hamsters, which, have been previously observed as components of hamster urine.[13] The confirmation of the resonance assignments of *p*-cresol-glucuronide, 4-hydroxy-3-methyl-phenylpropionic acid, and 2-aminoadipate were also aided by STOCSY (Figure 3). NMR resonance assignment of 2-aminoadipate was further confirmed

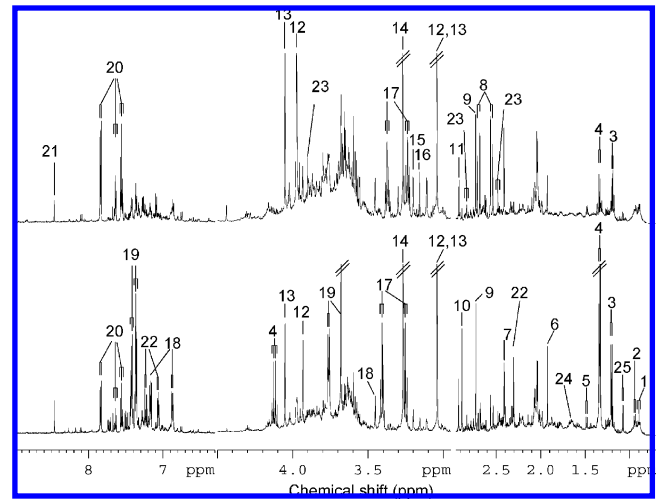

Figure 1. Representative 600 MHz ^{1}H NMR spectra obtained from urine of *N. americanus*-infected (bottom) and uninfected control (top) hamsters. Key: 1, butyrate; 2, 2-ketoisocaproate; 3, D-3-hydroxybutyrate; 4, lactate; 5, alanine; 6, acetate; 7, succinate; 8, citrate; 9, DMA; 10, TMA; 11, DMG; 12, creatine; 13, creatinine; 14, TMAO; 15, carnitine; 16, acetylcarnitine; 17, taurine; 18, 4-hydroxyphenylacetate; 19, PAG; 20, hippurate; 21, formate; 22, *p*-cresol-glucuronide; 23, 4-hydroxy-3-methylphenylpropionic acid; 24, 2-aminoadipate; 25, 3-hydroxyisobutyrate.

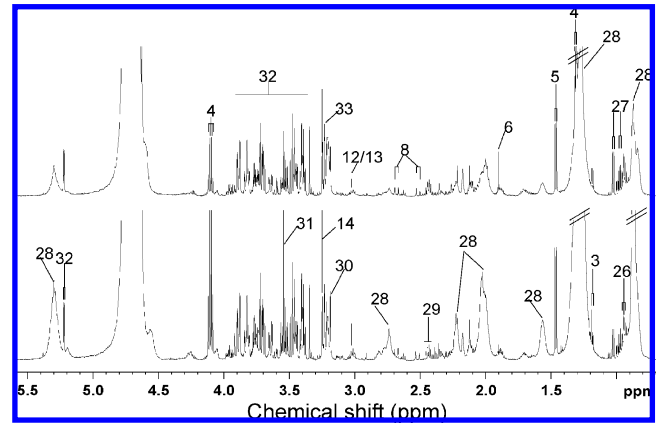

Figure 2. Representative 600 MHz ^{1}H NMR spectra of serum of *N. americanus*-infected (bottom) and uninfected control (top) hamsters. Key: 3, D-3-hydroxybutyrate; 4, lactate; 5, alanine; 6, acetate; 8, citrate; 12, creatine; 13, creatinine; 14, TMAO; 26, leucine; 27, valine; 28, lipoproteins; 29, glutamine; 30, choline; 31, glycine; 32, glucose; 33, phosphocholine.

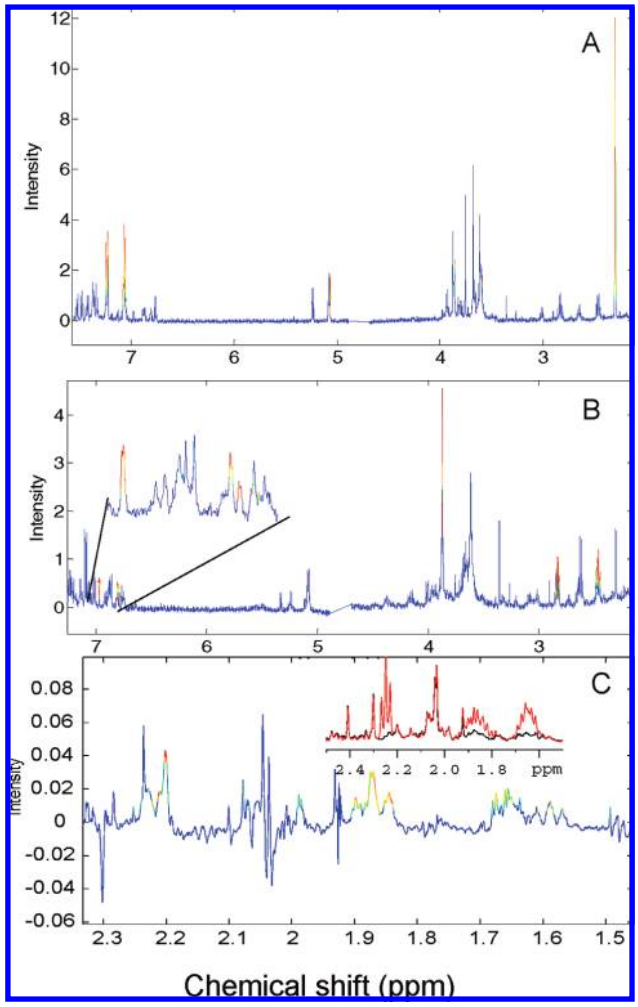

Figure 3. STOCSY obtained from urine of hamsters showing statistical connectivity of *p*-cresol-glucuronide (A), 4-hydroxy-3-methyl-phenylpropionic acid (B), and 2-aminoadipate (C). The inset represents NMR spectra obtained from a urine sample obtained from an infected hamster (black) and spiked with the standard of 2-aminoadipate (red). Of note, the correlation coefficient >0.7 is indicated in red color.

by spiking the standard of 2-aminoadipate into the urine sample (Figure 3C inset). In contrast to NMR spectra of urine samples, those obtained from serum contained fewer resolved signals and were intrinsically less variable due to homeostatic control of the blood composition and consisted of mainly leucine, valine, D-3-hydroxybutyrate, lactate, alanine, acetate, lipoproteins, citrate, glutamine, choline, glycine, creatine, creatinine, TMAO, glucose, and phosphocholine, which is consistent with the previous reports.[31,32]

Multivariate Data Analysis. PCA was initially performed on the spectra obtained from urine and serum samples using a mean centered unscaled data set in order to detect the presence of outliers that otherwise might distort the model interpretation. Overall, 6 urine spectra (among a total of 100 spectra) and 2 serum spectra (among a total of 20 spectra) were identified as being strong outliers. These outliers were caused by either insufficient water presaturation as a result of the samples being too diluted or were due to the presence of very high intensity peaks from lactate; hence, these samples were removed from subsequent analyses to avoid biasing the model. Pairwise comparisons between NMR spectra of urine from infected and uninfected control hamsters collected at matched time points, that is, preinfection, and days 1, 7, 21, and 35 postinfection were performed using an O-PLS-DA strategy. The same strategy was also applied to the NMR data obtained from serum of hamsters collected at the day of sacrifice, i.e., 35 days postinfection. NMR data were considered as the **X** matrix while classification information, i.e., infected or noninfected, as the dummy **Y** matrix. Unit variance scaling of the **X** matrix and 7-fold cross-validation were applied to the models. Parameters indicating the quality of these models, such as explained variance of the **X** matrix (R^2X) and predictivity (Q^2Y), were calculated, and *p*-values, corresponding to the significance of these models, were established (Table 1). Metabolic differences between control and infected hamsters were evident from just 1 day postinfection and became greater over time as demonstrated by the increased Q^2Y value calculated from the model. Although good separation between the NMR spectra of urine from the infected and the corresponding control hamsters was achieved for all sampling time points postinfection, as suggested by the values of the Q^2, the Q^2_{max} obtained from the permutation test (Table 1) was higher than that obtained from the real model for some of the time points, such as days 1, 7, and 21 postinfection. Since a higher Q^2 value could be obtained when randomizing classification information, this suggested that the model was unable to predict the sample class accurately and may therefore be overfitted at these time points. This would indicate that the infection is not metabolically well-characterized until after 21 days postinfection. However, models obtained from both urine and serum spectra at the end of the experiment were more predictive since the Q^2_{max} was equal to the real model.

Having performed validation of the O-PLS-DA models obtained from NMR spectra of serum and urine collected from *N. americanus*-infected and uninfected control hamsters, significant metabolic changes caused by the experimental infection were extracted from the corresponding PLS coefficient plots (Figure 4). The peaks pointing upward in the PLS coefficient plots indicate an increase in the relative concentrations of metabolites in the infected hamsters, while downward oriented peaks indicate an infection-induced decrease in metabolite concentrations. The color associated with each signal shows the significance of metabolites responsible for the separation as indicated by the color key depicting the r^2 values on the right-hand side of each coefficient plot. For the number of urine spectra included in the current analysis, a coefficient higher than 0.62 was regarded as being significant ($p < 0.05$) (Table 2). Here, only the infection discriminatory signals are listed. In some cases, the other resonances from the same molecule may not be significant due to overlap with other resonances derived from different molecules.

A number of urinary metabolites were found to reproducibly increase in infected hamsters, including PAG, *p*-cresol-glucuronide, and 2-aminoadipate. A corresponding decrease in the relative concentrations of hippurate, 4-hydroxyphenylactate, DMA, and 4-hydroxy-3-methyl-phenylpropionic acid was observed in the urine of *N. americanus*-infected hamsters. Although robust systematic changes in metabolic profiles were observed at day 35 postinfection, a trend toward changes in the levels of these metabolites was already detected at earlier time points (Figure 5). In the serum, the levels of lipoproteins and glycine were elevated in infected hamsters, whereas the concentrations of glucose, acetate, valine, leucine, and phosphocholine were found to be decreased at day 35 postinfection.

Table 1. Cross-Validation Parameters Generated from Multivariate Data Analysis[a]

	urine				serum
parameters	1 day postinfection	7 days postinfection	21 days postinfection	35 days postinfection	35 days postinfection
Q^2Y	0.63	0.39	0.76	0.93	0.85
Q^2_{max}	0.87	0.76	0.78	0.93	0.85
p-value	<0.001	0.05	<0.001	<0.001	<0.001
R^2X	0.32	0.38	0.29	0.43	0.36

[a] Q^2_{max} is generated from permutation test and when Q^2_{max} equals to Q^2Y, it is the case that classification for Q^2_{max} is the same as the classification for Q^2Y.

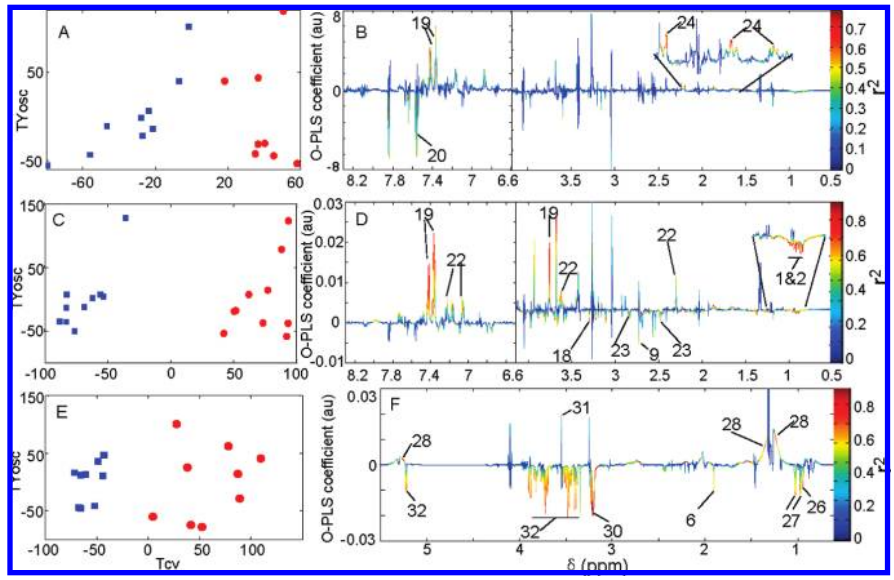

Figure 4. O-PLS-DA cross-validated scores plots obtained from ^{1}H NMR spectral data showing differentiation of the metabolic profiles of urine obtained from *N. americanus*-infected (red) and uninfected control (blue) hamsters at day 21 (A), day 35 postinfection (C) and serum obtained at day 35 postinfection (E). Each dot or box represents an individual sample. (B), (D), and (F) are the corresponding coefficient plots illustrating the important metabolites responsible for the variation. The coefficient plots were derived from back-transformed loadings from O-PLS-DA of unit variance ^{1}H NMR spectral data incorporated with coefficient scaled by the color on the right-hand side. Peaks pointing upward showed the increased metabolites and downward the decreased metabolites in the infected hamster, whereas colors are associated with the significance of metabolites. Key for metabolite identification is as in Figures 1 and 2.

To evaluate the presence of specific metabolites that correlated with the levels of worm burden, PLS models were constructed using NMR spectral data of urine and serum collected 35 days after infection as a respective **X** matrix and the worm burden as the **Y** matrix (Figure 6). Worm burden was positively associated with increased levels of urinary D-3-hydroxybutyrate and 3-hydroxyisobutyrate and serum lipoproteins, but negatively correlated with urinary hippurate and citrate. These observations are consistent with the results shown in Figure 4, where depleted levels of urinary hippurate and increased levels of serum lipoproteins were noted in infected hamsters.

Discussion

In the present study, a metabolic profiling strategy was utilized to elucidate the systems metabolic changes in the hamster due to an infection with the nematode *N. americanus*. We chose a Syrian SLAC hamster as an animal model because *N. americanus* is uniquely adapted to this host. Indeed, the parasite can survive in Syrian hamster without the need for immunosuppressive agents, which is an advantage compared to other animal models.[19] Perturbation of the urinary metabolite composition in infected hamsters was induced already 1 day postinfection and continued throughout the experiment, which lasted for 35 days. However, a permutation test performed on these models suggested that only the model generated from the urine obtained from the last time point, that is, 35 days after infection, was robustly predictive. The model obtained from NMR profiles of serum collected at sacrifice was also robust, based on both the Q^2 value and the permutation test. Larger groups of infected and uninfected control hamsters might have revealed significant differences in urinary metabolic profiles already at earlier time points postinfection, but in view of our previous experiences with similar samples sizes in other host-parasite models[12–18] and in light of the 3R rules (replace, reduce, and refine), a total of 10 hamsters per group was deemed an appropriate number.

In field epidemiologic investigations, a hookworm infection is usually diagnosed by microscopic examination of a fecal sample and the presence of eggs serves as the proof of an infection.[33] In humans, it takes 5−9 weeks from L_3 penetrating the unbroken skin to shedding hookworm eggs in feces; while, on average, it take 39 days in the hamster model.[34] In the current experimental study, we found systematic changes in metabolic profiles at day 35 postinfection, but detected trends in the same metabolites at earlier time points (Figure 5). Additionally, red blood cells were found to be markedly reduced at 5 weeks postinfection in hamsters.[34] Therefore, significant

Table 2. Changed Metabolites in Urine and Serum Due to an Infection with *N. americanus* in the Hamster Model

metabolites	δ (multiplicity)[a]	urine, 21 days postinfection $R^2X = 0.29$ $Q^2Y = 0.73$	urine, 35 days postinfection $R^2X = 0.43$ $Q^2Y = 0.87$	serum, 35 days postinfection $R^2X = 0.37$ $Q^2Y = 0.84$
butyrate	0.89 (t)		−0.82	
2-ketoisocaproate	0.92 (d)		−0.87	
DMA	2.73 (s)		−0.73	
UN1	3.22 (s)		−0.83	
UN2	3.11 (s)	−0.71	−0.79	
4-hydroxyphenylacetate	3.30 (s)		−0.88	
creatine	3.93 (s)		+0.75	
p-cresol-glucuronide	7.05 (d)		+0.77	
4-hydroxy-3-methyl-phenylpropionic acid	2.46 (t)		−0.71	
	2.82 (t)			
2-aminoadipate	2.20 (m) 1.87 (m)	+0.80	+0.91	
	1.65 (m)			
PAG	7.37 (t)	+0.77	+0.86	
hippurate	7.63 (t)	−0.62		
leucine	0.95 (t)			−0.89
valine	1.03 (d)			−0.82
lipoproteins	5.26 (b)			+0.78
acetate	1.91 (s)			−0.75
glycine	3.55 (s)			+0.63
glucose	5.23 (d)			−0.79
phosphocholine	3.21 (s)			−0.94

[a] Only the discriminatory signals are listed. + and −: indicate the presence of increased (+) or decreased (−) levels of metabolite followed with infection; s, singlet; d, doublet; t: triplet; m, multiplet; b, broad peak. UN: denoted as unknown.

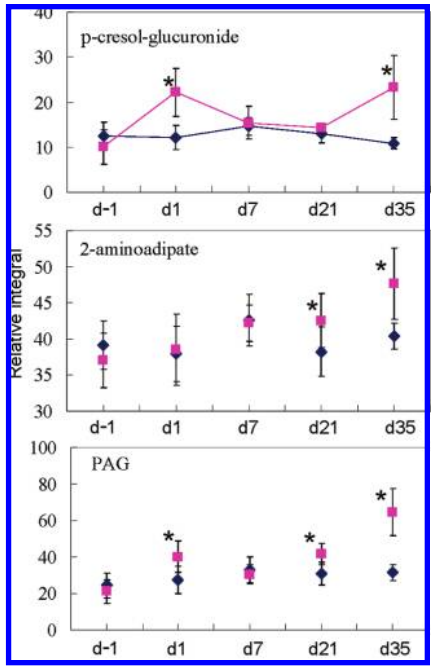

Figure 5. The averaged relative NMR intensities of ρ-cresol-glucuronide, 2-aminoadipate and PAG in urine obtained from *N. americanus*-infected (pink solid squares) and uninfected control hamsters (black solid diamonds). Bar denoted the standard deviations of the metabolite at given time point and *t* test performed on these metabolites indicated that the metabolites marked with an asterisk were different between control and infected hamsters at a significance level of $p < 0.05$.

changes in the metabolic profiles of infected hamsters 5 weeks after infection coincide with the maturation of *N. americauns* and onset of egg production. One of the prominent changes induced by a *N. americanus* infection in the hamster was the alteration of host energy-related metabolism, which is reflected in the increased concentration of lipoprotein lipids and decreased concentration of blood glucose. Adult hookworms attach to the intestinal mucosa and suck blood, which causes malnutrition and anemia,[5] leading to alterations of energy metabolism of the host. Previously, malabsorption of sugars has been noted in patients with hookworm infections,[35,36] and increase in free fatty acids and decrease in liver glycogen have also been observed in hookworm-infected hamsters.[37] The same investigation also noted an abnormal glucose tolerance level, which has been attributed to anemia and stress consequential to the development of an infection. Additionally, we also observed decreased levels of branched chain amino acids (BCAAs), such as valine and leucine in the serum of infected hamsters. These amino acids are ketogenic amino acids, and capable of producing keto acids, such as 2-ketoisovalerate and 2-ketoisocaproate *via* aminotransferases.[38] These keto acids could also be further metabolized into acetyl-CoA, which may contribute to the depletion of urinary 2-ketoisocaproate observed in the infected hamsters.

In the present investigation, we found increased levels of 2-aminoadipate in the urine of *N. americanus*-infected hamsters (Table 2), which is a unique 'biomarker' relative to all the other parasite-host models we have investigated thus far.[12–18] Of note, 2-aminoadipate is an important intermediate of catabolism of lysine *via* bacteria such as *Streptomyces* spp. and *Pseudomonas putida*.[39,40] 2-aminoadipate is the best-described gliotoxin in the field of neuroscience[41] and has previously been found to be destructive to Muller cells after an injection of 2-aminoadipate to rats.[42] It has also been shown to change brain structure as indicated by invasion of astrocytes and presence of large number of microglia.[43] In human, elevated levels of 2-aminoadipate has been found in infants with metabolic disease, which is caused by a defect in the oxidative decarboxylation of 2-oxoadipate, a catabolic intermediate of lysine, tryptophan, and hydroxylysine.[44] It has been previously reported that 5 out of 7 children with an elevated level of 2-aminoadipate presented with psychomotor retardation.[45] Additionally, 2-aminoadipate has been shown to relate to neurological disorders, such as seizures and convulsions.[46]

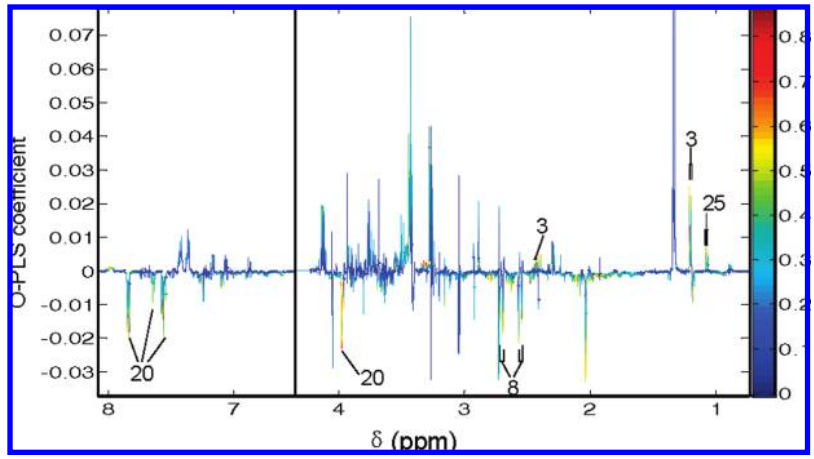

Figure 6. The coefficient plot illustrates the correlation between urinary metabolites and worm burden. The plot was derived from O-PLS analysis using unit variance scaled ^{1}H NMR spectral data as the **X** matrix and worm burden as **Y** variable. The upward oriented peaks indicate a positive correlation with worm burden and downward oriented peaks a negative correlation. For metabolite key, see caption for Figure 1.

Likewise, this metabolite has also been found in increased concentrations in the urine of experimental animals treated with the steatotic hepatotoxin hydrazine.[47] In addition to overt liver toxicity, hydrazine has also been shown to induce convulsions and seizures in some animals and is thought to have central nervous system (CNS) toxicity.[47]

One of the pathological manifestations of hookworm infection is impairment of cognitive function in children. The elevated level of 2-aminoadipate found in *N. americanus*-infected hamsters may, therefore, be related to the neurological consequences of a hookworm infection. However, severe malnutrition attributed to anemia caused by this parasite is an another likely explanation of this observation.[48] To further investigate whether 2-aminoadipate is a potentially marker of hookworm infection in humans, it would be interesting to characterize the urinary metabolic profiles of hookworm-infected patients and compare the results with noninfected controls, placing particular emphasis on the presence and level of 2-aminoadipate.

At present, the origin of the elevation of 2-aminoadipate in *N. americanus*-infected hamster is unclear. Further, ^{1}H NMR spectra obtained from *N. americanus* worms and its extract failed to show the presence of 2-aminoadipate (data not shown). Alternatively, since bacteria are capable of producing 2-aminoadipate, it is conceivable that the elevated level of 2-aminoadipate found among infected hamsters may indicate an alteration of microbiota composition and activity. Further evidence supporting this hypothesis derives from the urinary metabolic profiles of *N. americanus*-infected hamsters. For example, urinary concentrations of 4-hydroxy-3-methylphenylpropionic acid, hippurate, and 4-hydroxyphenylactate were depleted. Moreover, the level of hippurate was found to be negatively correlated with overall worm burden. Hydroxyphenylactate and phenylpropionic acid are products of degradation of different dietary flavonoids by colonic microbiota, and once absorbed, these acids undergo β-oxidation and glycination in the liver to form hippurate prior to excretion *via* the urine.[49] The fact that the dietary regime was kept the same throughout the experiment suggests depletions of these aromatic compounds were due to the fluctuations of the presence or activity of the host gut microbiota. In previous studies, hippurate and hydroxyphenyl propionic acid excretions were shown to be correlated with the microfloral composition of the host colon.[50,51] The fact that DMA, which is derived from choline *via* gut microbiota,[52] was also found to be depleted in the urine of *N. americanus*-infected hamsters is consistent with the disrupted microflora theory.

Additionally, elevated levels of *p*-cresol-glucuronide were observed in the urine of infected hamsters. *p*-cresol-glucuronide is generated from *p*-cresol *via* liver phase II detoxification mechanism and *p*-cresol has been shown to be elevated in the urine of mice infected with *S. mansoni*[12] and hamsters infected with *S. japonicum*.[13] Thus far, 2 *Clostridium* subspecies, *Clostridium difficile* and *Clostridium scatologens*, are reported to produce *p*-cresol.[53,54] Furthermore, elevated concentrations of PAG were also noted in the urine of *N. americanus*-infected hamsters. This observation has also been made in the previous investigations of metabolic responses of murines infected with *Schistosoma* spp.[12,13] The increased concentration of PAG in the urine has been reported to occur as a consequence of the drug-induced phospholipidosis,[55] but also been proposed to be attributed to variability in the gut microbiota.[50] Moreover, a reduction in the concentrations of SCFAs, such as acetate and butyrate, was observed in the urine samples obtained from *N. americanus*-infected hamsters. These SCFAs are produced by bacteria through fermentation of unabsorbed dietary fibres. All the changed metabolites in the urine of infected hamsters mentioned above suggest an alteration of activities or populations of gut microbiota. This is not surprising since adult *N. americanus* worms reside in the intestine of their host, and hence live in close proximity with gut microbiota and therefore are connected either by direct chemical interaction or by modification of resources. It is therefore expected that a hookworm infection impacts on the gut microbiota. Parasitic infections alter the activities or composition of gut microbiota, which appears to be a general phenomenon and has been documented before for protozoa (*P. berghei* and *T. brucei brucei*),[17,18] and different kinds of parasitic worms (*S. mansoni*, *S. japonicum*, and *E. caproni*).[12–15] Thus far, it is not known whether a *N. americanus* infection affects the gut microbiota of mice, hamsters and, indeed, humans in the same way. It is also not known whether specific species of gut microbiota are being particularly affected by a

N. americanus infection. Hence, further in-depth microbiotal investigations are warranted in host−parasite model.

In conclusion, a *N. americanus* infection in the hamster caused alteration of energy metabolism, disturbance of the gut microbiota, and an elevated urinary excretion of 2-aminoadipate, which thus far is a unique descriptor for this host−parasite model and provides a testable hypothesis that requires follow-up investigation in humans. Our results underscore that a metabolic profiling approach is useful to derive global metabolic responses of host animals to a parasite infection. A deeper understanding of this phenomenon and of the more general role of the gut microbiota in the metabolic expression of the infection will further enhance our current knowledge of the mechanism of hookworm infection and disease.

Acknowledgment. This study received financial support from the Chinese Academy of Science (KJXC2-YW-W11) and partial financial support from the National Institute of Parasitic Diseases, Chinese Center for Disease Control and Prevention. J. Utzinger is grateful to the Swiss National Science Foundation for financial support (project no. PPOOB-102883, PPOOB-119129).

References

(1) Bethony, J.; Brooker, S.; Albonico, M.; Geiger, S. M.; Loukas, A.; Diemert, D.; Hotez, P. J. Soil-transmitted helminth infections: ascariasis, trichuriasis, and hookworm. *Lancet* **2006**, *367* (9521), 1521–1532.

(2) Hotez, P. J.; Molyneux, D. H.; Fenwick, A.; Ottesen, E.; Ehrlich Sachs, S.; Sachs, J. D. Incorporating a rapid-impact package for neglected tropical diseases with programs for HIV/AIDS, tuberculosis, and malaria. *PLoS Med.* **2006**, *3* (5), e102.

(3) Bungiro, R.; Cappello, M. Hookworm infection: new developments and prospects for control. *Curr. Opin. Infect. Dis.* **2004**, *17* (5), 421–426.

(4) Brooker, S.; Clements, A. C. A.; Bundy, D. A. P. Global epidemiology, ecology and control of soil-transmitted helminth infections. *Adv. Parasitol.* **2006**, *62*, 221–261.

(5) Hotez, P. J.; Brooker, S.; Bethony, J. M.; Bottazzi, M. E.; Loukas, A.; Xiao, S. H. Hookworm infection. *N. Engl. J. Med.* **2004**, *351* (8), 799–807.

(6) Hotez, P. J. Hookworm disease in children. *Pediatr. Infect. Dis. J.* **1989**, *8* (8), 516–520.

(7) de Silva, N. R. Impact of mass chemotherapy on the morbidity due to soil-transmitted nematodes. *Acta Trop.* **2003**, *86* (2−3), 197–214.

(8) Keiser, J.; Utzinger, J. Efficacy of current drugs against soil-transmitted helminth infections - systematic review and meta-analysis. *JAMA* **2008**, *299* (16), 1937–1948.

(9) Stiles, C. W. Early history, in part esoteric, of the hookworm (Ucinariasis) campaign in our Southern United States. *J. Parasitol.* **1939**, *25* (4), 283–308.

(10) Hotez, P. J.; Bethony, J. M.; Oliveira, S. C.; Brindley, P. J.; Loukas, A. Multivalent anthelminthic vaccine to prevent hookworm and schistosomiasis. *Expert Rev. Vaccines* **2008**, *7* (6), 745–752.

(11) Nicholson, J. K.; Lindon, J. C.; Holmes, E. 'Metabonomics': understanding the metabolic responses of living systems to pathophysiological stimuli via multivariate statistical analysis of biological NMR spectroscopic data. *Xenobiotica* **1999**, *29* (11), 1181–1189.

(12) Wang, Y. L.; Holmes, E.; Nicholson, J. K.; Cloarec, O.; Chollet, J.; Tanner, M.; Singer, B. H.; Utzinger, J. Metabonomic investigations in mice infected with *Schistosoma mansoni*: an approach for biomarker identification. *Proc. Natl. Acad. Sci. U.S.A.* **2004**, *101* (34), 12676–12681.

(13) Wang, Y. L.; Utzinger, J.; Xiao, S. H.; Xue, J.; Nicholson, J. K.; Tanner, M.; Singer, B. H.; Holmes, E. System level metabolic effects of a *Schistosoma japonicum* infection in the Syrian hamster. *Mol. Biochem. Parasitol.* **2006**, *146* (1), 1–9.

(14) Saric, J.; Li, J. V.; Wang, Y. L.; Keiser, J.; Veselkov, K. A.; Dirnhofer, S.; Yap, I. K. S.; Nicholson, J. K.; Holmes, E.; Utzinger, J. Panorganismal metabolic response modelling of an experimental *Echinostoma caproni* infection in the mouse. *J. Proteome Res.* **2009**, *8* (8), 3899–3911.

(15) Saric, J.; Li, J. V.; Wang, Y. L.; Keiser, J.; Bundy, J. G.; Holmes, E.; Utzinger, J. Metabolic profiling of an *Echinostoma caproni* infection in the mouse for biomarker discovery. *PLoS Negl. Trop. Dis.* **2008**, *2* (7), e254.

(16) Martin, F. P. J.; Verdu, E. F.; Wang, Y. L.; Dumas, M. E.; Yap, I. K. S.; Cloarec, O.; Bergonzelli, G. E.; Corthesy-Theulaz, I.; Kochhar, S.; Holmes, E.; Lindon, J. C.; Collins, S. M.; Nicholson, J. K. Transgenomic metabolic interactions in a mouse disease model: interactions of *Trichinella spiralis* infection with dietary *Lactobacillus paracasei* supplementation. *J. Proteome Res.* **2006**, *5* (9), 2185–2193.

(17) Wang, Y. L.; Utzinger, J.; Saric, J.; Li, J. V.; Burckhardt, J.; Dirnhofer, S.; Nicholson, J. K.; Singer, B. H.; Brun, R.; Holmes, E. Global metabolic responses of mice to *Trypanosoma brucei brucei* infection. *Proc. Natl. Acad. Sci. U.S.A.* **2008**, *105* (16), 6127–6132.

(18) Li, J. V.; Wang, Y. L.; Saric, J.; Nicholson, J. K.; Dirnhofer, S.; Singer, B. H.; Tanner, M.; Wittlin, S.; Holmes, E.; Utzinger, J. Global metabolic responses of NMRI mice to an experimental *Plasmodium berghei* infection. *J. Proteome Res.* **2008**, *7* (9), 3948–3956.

(19) Xue, J.; Xiao, S.; Qiang, H.; Liu, S.; Hotez, P.; Shen, B.; Xue, H.; Li, T.; Zhan, B. *Necator americanus*: maintenance through one hundred generations in golden hamsters (*Mesocricetus auratus*). II. Morphological development of the adult and its comparison with humans. *Exp. Parasitol.* **2003**, *105* (3−4), 192–200.

(20) Meiboom, S.; Gill, D. Modified spin-echo method for measuring nuclear relaxation times. *Rev. Sci. Instrum.* **1958**, *29*, 688–691.

(21) Hurd, R. E. Gradient-enhanced spectroscopy. *J. Magn. Reson.* **1990**, *87* (2), 422–428.

(22) Bax, A.; Davis, D. G. MLEV-17-based two-dimensional homonuclear magnetization transfer spectroscopy. *J. Magn. Reson.* **1985**, *65* (2), 355–360.

(23) Beckwith-Hall, B. M.; Brindle, J. T.; Barton, R. H.; Coen, M.; Holmes, E.; Nicholson, J. K.; Antti, H. Application of orthogonal signal correction to minimise the effects of physical and biological variation in high resolution ^{1}H NMR spectra of biofluids. *Analyst* **2002**, *127* (10), 1283–1288.

(24) Wold, S.; Antti, H.; Lindgren, F.; Ohman, J. Orthogonal signal correction of near-infrared spectra. *Chemom. Intell. Lab.* **1998**, *44* (1−2), 175–185.

(25) Trygg, J. O2-PLS for qualitative and quantitative analysis in multivariate calibration. *J. Chemom.* **2002**, *16* (6), 283–293.

(26) Wold, S.; Ruhe, A.; Wold, H.; Dunn, W. J. The collinearity problem in linear-regression—the partial least-squares (PLS) approach to generalized inverses. *J. Sci. Stat. Comput.* **1984**, *5* (3), 735–743.

(27) Cloarec, O.; Dumas, M. E.; Trygg, J.; Craig, A.; Barton, R. H.; Lindon, J. C.; Nicholson, J. K.; Holmes, E. Evaluation of the orthogonal projection on latent structure model limitations caused by chemical shift variability and improved visualization of biomarker changes in ^{1}H NMR spectroscopic metabonomic studies. *Anal. Chem.* **2005**, *77* (2), 517–526.

(28) Westerhuis, J. A.; Hoefsloot, H. C. J.; Smit, S.; Vis, D. J.; Smilde, A. K.; van Velzen, E. J. J.; van Duijnhoven, J. P. M.; van Dorsten, F. A. Assessment of PLSDA cross validation. *Metabolomics* **2008**, *4* (1), 81–89.

(29) Nicholson, J. K.; Foxall, P. J. D.; Spraul, M.; Farrant, R. D.; Lindon, J. C. 750-MHz ^{1}H and ^{1}H-^{13}C NMR spectroscopy of human blood-plasma. *Anal. Chem.* **1995**, *67* (5), 793–811.

(30) Cloarec, O.; Dumas, M. E.; Craig, A.; Barton, R. H.; Trygg, J.; Hudson, J.; Blancher, C.; Gauguier, D.; Lindon, J. C.; Holmes, E.; Nicholson, J. Statistical total correlation spectroscopy: an exploratory approach for latent biomarker identification from metabolic ^{1}H NMR data sets. *Anal. Chem.* **2005**, *77* (5), 1282–1289.

(31) Wang, Y. L.; Holmes, E.; Tang, H. R.; Lindon, J. C.; Sprenger, N.; Turini, M. E.; Bergonzelli, G.; Fay, L. B.; Kochhar, S.; Nicholson, J. K. Experimental metabonomic model of dietary variation and stress interactions. *J. Proteome Res.* **2006**, *5* (7), 1535–1542.

(32) Wang, Y. L.; Lawler, D.; Larson, B.; Ramadan, Z.; Kochhar, S.; Holmes, E.; Nicholson, J. K. Metabonomic investigations of aging and caloric restriction in a life-long dog study. *J. Proteome Res.* **2007**, *6* (5), 1846–1854.

(33) Bergquist, R.; Johansen, M. V.; Utzinger, J. Diagnostic dilemmas in helminthology: what tools to use and when. *Trends Parasitol.* **2009**, *25* (4), 151–156.

(34) Xue, J.; Qiang, H. Q.; Yao, J. M.; Fujiwara, R.; Zhan, B.; Hotez, P.; Xiao, S. H. *Necator americanus*: optimization of the golden hamster model for testing anthelmintic drugs. *Exp. Parasitol.* **2005**, *111* (4), 219–223.

(35) Falaiye, J. M.; Oladapo, J. M.; Wali, S. S. Hookworm enteropathy. *J. Trop. Med. Hyg.* **1974**, *77* (9), 211–214.

(36) Tandon, B. N.; Kohli, R. K.; Saraya, A. K.; Ramachan, K.; Prakash, O. Role of parasites in pathogenesis of intestinal malabsorption in hookworm disease. *Gut* **1969**, *10* (4), 293–298.

(37) Kaul, C. L.; Talwalker, P. K.; Sen, H. G.; Grewal, R. S. Changes in carbohydrate-metabolism in golden hamsters infected with *Necator americanus*. *Ann. Trop. Med. Parasitol.* **1982**, *76* (4), 475–482.
(38) Cynober, L. A. *Metabolic and Therapeutic Aspects of Amino Acids in Clinical Nutrition*; Cynober L.A CRC Press: London, 2004.
(39) Madduri, K.; Stuttard, C.; Vining, L. C. Lysine catabolism in *Streptomyces* spp is primarily through *Cadaverine-β*-lactam producers also make α-aminoadipate. *J. Bacteriol.* **1989**, *171* (1), 299–302.
(40) Revelles, O.; Wittich, R. M.; Ramos, J. L. Identification of the initial steps in D-lysine catabolism in *Pseudomonas putida*. *J. Bacteriol.* **2007**, *189* (7), 2787–2792.
(41) Billet, F.; Costentin, J.; Dourmap, N. Influence of glial cells in the dopamine releasing effect resulting from the stimulation of striatal delta-opioid receptors. *Neuroscience* **2007**, *150* (1), 131–143.
(42) Pedersen, O. O.; Karlsen, R. L. Destruction of Muller cells in the adult rat by intravitreal injection of D,L-alpha-aminoadipic acid—electron-microscopic study. *Exp. Eye Res.* **1979**, *28* (5), 569–575.
(43) Takada, M.; Hattori, T. Fine structural changes in the rat-brain after local injections of gliotoxin, alpha-aminoadipic acid. *Histol Histopathol* **1986**, *1* (3), 271–275.
(44) Przyrembel, H.; Bachmann, D.; Lombeck, I.; Becker, K.; Wendel, U.; Wadman, S. K.; Bremer, H. J. α-ketoadipic aciduria, a new inborn error of lysine metabolism—biochemical studies. *Clin. Chim. Acta* **1975**, *58* (3), 257–269.
(45) Peng, H.; Shinka, T.; Inoue, Y.; Mitsubuchi, H.; Ishimatsu, J.; Yoshino, M.; Kuhara, T. Asymptomatic alpha-ketoadipic aciduria detected during a pilot study of neonatal urine screening. *Acta Paediatr.* **1999**, *88* (8), 911–914.
(46) Jakobs, C.; Degrauw, A. J. C. A fatal case of 2-ketoadipic, 2-hydroxyadipic and 2-aminoadipic aciduria—relation of organic aciduria to phenotype. *J. Inherited Metab. Dis.* **1992**, *15* (2), 279–280.
(47) Nicholls, A. W.; Holmes, E.; Lindon, J. C.; Shockcor, J. P.; Farrant, R. D.; Haselden, J. N.; Damment, S. J. P.; Waterfield, C. J.; Nicholson, J. K. Metabonomic investigations into hydrazine toxicity in the rat. *Chem. Res. Toxicol.* **2001**, *14* (8), 975–987.
(48) Bergen, D. Effects of poverty on cognitive function: a hidden neurologic epidemic. *Neurology* **2008**, *71* (6), 447–451.
(49) Rechner, A. R.; Kuhnle, G.; Bremner, P.; Hubbard, G. P.; Moore, K. P.; Rice-Evans, C. A. The metabolic fate of dietary polyphenols in humans. *Free Radical Biol. Med.* **2002**, *33* (2), 220–235.
(50) Nicholls, A. W.; Mortishire-Smith, R. J.; Nicholson, J. K. NMR spectroscopic-based metabonomic studies of urinary metabolite variation in acclimatizing germ-free rats. *Chem. Res. Toxicol.* **2003**, *16* (11), 1395–1404.
(51) Williams, R. E.; Eyton-Jones, H. W.; Farnworth, M. J.; Gallagher, R.; Provan, W. M. Effect of intestinal microflora on the urinary metabolic profile of rats: a ^{1}H nuclear magnetic resonance spectroscopy study. *Xenobiotica* **2002**, *32* (9), 783–794.
(52) Zeisel, S. H.; Wishnok, J. S.; Blusztajn, J. K. Formation of methylamines from ingested choline and lecithin. *J. Pharmacol. Exp. Ther.* **1983**, *225* (2), 320–324.
(53) Yu, L.; Blaser, M.; Andrei, P. I.; Pierik, A. J.; Selmer, T. 4-hydroxyphenylacetate decarboxylases: properties of a novel subclass of glycyl radical enzyme systems. *Biochemistry* **2006**, *45* (31), 9584–9592.
(54) Selmer, T.; Andrei, P. I. p-hydroxyphenylacetate decarboxylase from *Clostridium difficile*—a novel glycyl radical enzyme catalysing the formation of *p*-cresol. *Eur. J. Biochem.* **2001**, *268* (5), 1363–1372.
(55) Delaney, J.; Neville, W. A.; Swain, A.; Miles, A.; Leonard, M. S.; Waterfield, C. J. Phenylacetylglycine, a putative biomarker of phospholipidosis: its origins and relevance to phospholipid accumulation using amiodarone treated rats as a model. *Biomarkers* **2004**, *9* (3), 271–290.

PR900711J